Case Studies in Thermal Engineering 28 (2021) 101628

Contents lists available at ScienceDirect

Case Studies in Thermal Engineering

journal homepage: www.elsevier.com/locate/csite

Combustion process of nanofluids consisting of oxygen molecules and aluminum nanoparticles in a copper nanochannel using molecular dynamics simulation

Heng Chen [a,b,**], Dmitry Bokov [c], Supat Chupradit [d], Maboud Hekmatifar [e], Mustafa Z. Mahmoud [f,g], Roozbeh Sabetvand [h], Jinying Duan [b], Davood Toghraie [e,*]

[a] Shaanxi Engineering Research Center of Controllable Neutron Source, Xijing University, Xi'an, Shaanxi, 710123, China
[b] School of Science, Xijing University, Xi'an, Shaanxi, 710123, China
[c] Institute of Pharmacy, Sechenov First Moscow State Medical University, 8 Trubetskaya St., Bldg. 2, Moscow, 119991, Russian Federation
[d] Department of Occupational Therapy, Faculty of Associated Medical Sciences, Chiang Mai University, Chiang Mai, 50200, Thailand
[e] Department of Mechanical Engineering, Khomeinishahr Branch, Islamic Azad University, Khomeinishahr, Iran
[f] Department of Radiology and Medical Imaging, College of Applied Medical Sciences, Prince Sattam Bin Abdulaziz University, Al-Kharj, 11942, Saudi Arabia
[g] Faculty of Health, University of Canberra, Canberra, ACT, Australia
[h] Department of Energy Engineering and Physics, Faculty of Condensed Matter Physics, Amirkabir University of Technology, Tehran, Iran

ARTICLE INFO

Keywords:
Nanofluid
Combustion
Molecular dynamics
Temperature
Pressure
Heat flux
Nanoparticles

ABSTRACT

Investigation of the combustion process in nanofluids consisting of oxygen molecules and aluminum nanoparticles indicates the factors affecting this process and, as a result, creates a phase change in the simulated atomic structure. In this study, using molecular dynamics simulations, the combustion process in nanofluids, including oxygen molecules and aluminum nanoparticles, was studied from an atomic point of view. The physical equilibrium in atomic samples was initially investigated by examining atomic structures' kinetic energy and potential energy. Kinetic energy and potential energy were balanced at 77.02 eV and −6769.58 eV, respectively. This convergence in the expressed physical quantities indicated that the atomic structure of the prototype and the interaction between the atomic structures were well selected. Also, some factors such as changes in initial temperature and pressure and the change in applied external heat flux to the nanofluid led to the optimal conditions for combustion in the atomic structure and processes such as heat transfer. As the initial temperature rises to 400 K, the flux in the atomic sample and the combustion time converged to 1289 Wm^{-2} and 6.29 ns, respectively. And with increasing pressure in atomic samples to 6 bar, atomic oscillations decrease. Also, the flowing flux in the atomic sample and the combustion time converged to 1383 Wm^{-2} and 5.5.31 ns with increasing external heat flux.

* Corresponding author.
** Corresponding author. Shaanxi Engineering Research Center of Controllable Neutron Source, Xijing University, Xi'an, Shaanxi, 710123, China.
E-mail addresses: chenheng@xijing.edu.cn (H. Chen), Toghraee@iaukhsh.ac.ir (D. Toghraie).

https://doi.org/10.1016/j.csite.2021.101628
Received 19 June 2021; Received in revised form 20 October 2021; Accepted 5 November 2021
Available online 6 November 2021

1. Introduction

Nanotechnology is an interdisciplinary science related to medical and therapeutic fields up to industrial devices and various science and engineering disciplines [1]. Nanostructure refers to structures that have at least one dimension less than 100 nm [2–5]. Combustion is a reaction in which a substance combines with oxygen very quickly, and in addition to producing oxygenated compounds, heat and light are also produced in this process [6]. Combustion of fossil fuels leads to the production of significant pollutants and, ultimately, global warming due to the formation of elements such as NO_X, CO, and CO_2 [7]. According to recent research and the importance of industry in the production of pollutants and damage to the environment, the study of geometric parameters in the operation of industrial combustion bins requires further and more complete study. Several experimental and computational methods and computer simulations in combustion in atomic nanostructures were performed in previous studies.

In the continuation of this section, a number of these studies are discussed. In a study, Jung et al. [8] investigated the effect of the addition of Ce nanoparticles on the combustion process in diesel fuel. They reported that the oxidation rate and combustion temperature increase and decrease by adding this nanoparticle, respectively. Kong et al. [9] examined nickel compounds' thermal behaviors and combustion in the polypropylene/IFR system. They reported that these nanoparticles improved the combustion process and reduced the amount of smoke production. Allen et al. [10] studied the combustion of liquid fuels by increasing nanoparticles. The results showed that adding Al nanoparticles reduces the combustion delay by up to 32%. In an experimental study, Sun et al. [11] investigated the effect of diameter and concentration of Al nanoparticles on the combustion process of liquid fuels. They reported that the increase in nanoparticles led to an increase in flame emission. Tyagi et al. [12] examined the effect of adding Al nanoparticles to diesel fuel on combustion. Nanoparticles were studied in volume fractions of 0, 0.1 and 0.5%. They reported that increasing Al volume fraction increases the hot spots inside the bin and allows ignition from several points.

In a computational study using molecular dynamics, Hong et al. [13] investigated the combustion process in aluminum nanoparticles. This study was performed at different initial temperatures as well as different oxygen densities in the simulation box. This study showed the proper combustion process and significant adsorption of oxygen molecules by simulated aluminum nanoparticles in different temperature ranges and oxygen density in the simulation box. In a computational study, Li et al. [14] examined the combustion behavior of aluminum nanoparticles. This research group showed that a molecular dynamics method is suitable for studying aluminum-based atomic structures' thermal and combustion behavior. In a computational study based on quantum theory, Bayout et al. [15] examined the combustion behavior of aluminum nanoparticles. In their research, this research group used simulations of density functional theory. It showed that the appropriate temperature for creating an optimal combustion process in aluminum nanoparticles is equal to 3500 K. Bidabadi et al. [16] examined the combustion process of Al microparticles in a filled box with oxygen molecules. The molecular dynamics simulations show these microparticles' adsorption of oxygen molecules and combustion processes in a wide temperature range. The present study investigates the combustion process in a copper nanoparticle with nanofluid, including oxygen molecules and aluminum nanoparticles. In general, in the simulated sample, aluminum nanoparticles with a radius of 5 nm and the dimensions of the simulation box are assumed to be $10 \times 10 \times 15\ nm^3$. The created total temperature in the structures equals 300 K, the initial pressure equals 1 bar, and the atomic percentage of aluminum nanoparticles is considered 1%. Fig. 1 shows a simulated atomic structure by the molecular dynamics method. In general, in this study, we investigate the effect of temperature and initial pressure and external heat flux on the combustion of atomic structures.

2. Computational method

Molecular dynamics simulation is a method that can predict the temporal evolution of a system consisting of interacting particles (atoms, molecules, granules, etc.) and thus estimate the associated physical properties [17]. In MD simulation, the time course of particle interactions of a system is studied using Newton's second law as follows [18]:

$$F_i = \sum_{i \neq j} F_{ij} = m_i \frac{d^2 r_i}{dt^2} = m_i \frac{dv_i}{dt} \tag{1}$$

The approximate numerical computational method for advancing the system by one-time step is called the integral algorithm. In

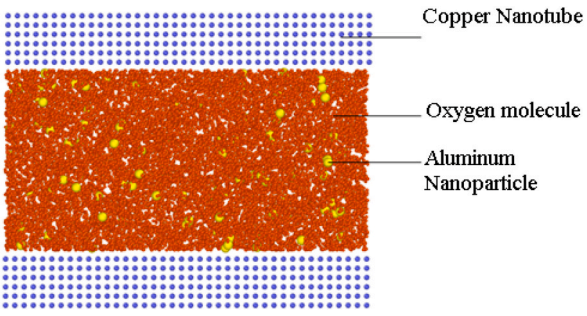

Fig. 1. A view of the simulated atomic structure using LAMMPS software.

the molecular dynamics of continuous potentials, the classical motion equations are determined using finite difference algorithms and lead to calculating molecular locations and velocities in equal time sequences. Accuracy, stability, simplicity, speed, and economic aspects are important in choosing an algorithm. Among the integration algorithms, velocity-Verlet is the most common type. The velocity-Verlet algorithm is estimated with these equations [19]:

$$r_i(t+\Delta t) = r_i(t) + \Delta t\, v_i(t) + \frac{\Delta t^2 a_i\,(t)}{2} \tag{2}$$

$$a_i(t+\Delta t) = \frac{F_i\,(t+\Delta t)}{m_i} \tag{3}$$

$$v_i(t+\Delta t) = v_i(t) + \Delta t\, a_i(t) + \frac{\Delta t\,(a_i\,(t) + a_i(t+\Delta t))}{2} \tag{4}$$

In these equations, $a_i(t\ +\ \Delta t)$, $v_i(t\ +\ \Delta t)$, $r_i(t\ +\ \Delta t)$, and $a_i(t)$, $v_i(t)$, $r_i(t)$ show the acceleration of particles, velocity, and initial and final position. In general, the main purpose of simulating systems containing large numbers of particles is to obtain mass properties mainly defined by the location of the nuclei of atoms. Therefore, a logical approximation and based on physics from the force field (potential function) can make a suitable inference about the system's behavior. To evaluate the total potential energy, the applied non-bonded and bonded interactions to the particles must be summed [20]:

$$E_{total} = E_{bonded} + E_{nonbonded} \tag{5}$$

The Lennard-Jones potential is a simple mathematical model that approximates the interactions between a pair of neutral atoms or molecules. The most common formulation for the Lennard-Jones potential function is expressed as Eq. (6) [21]:

$$U_{LJ} = 4\varepsilon\left[\left(\frac{\sigma}{r}\right)^{12} - \left(\frac{\sigma}{r}\right)^{6}\right] \tag{6}$$

In this equation, ε is the size of the potential well, r_c in this formulation represents the potential cut-off radius, and σ is the distance at which the potential becomes zero. Electrical potential energy or electrostatic potential energy is obtained from the Coulombic steady forces [22,23]. This energy determines the amount of force of static electric charges on the particles of a system that absorb and repel each other. Electric potential energy is defined according to Eq. (7) [22]:

$$\mathrm{U(r)} = \frac{-1}{4\pi\varepsilon_0}\frac{\mathrm{q_1 q_2}}{\mathrm{r^2}} \tag{7}$$

In the above relation, r is the distance between the charges, q_1 and q_2 are electric charges, and ε_0 indicates the electrical permeability of the open space. The EAM potential function is used to calculate the interaction of metal particles. This equation is represented as follow [18,24]:

$$U_i = F_\alpha\left(\sum_{i\neq j}\rho_\beta(r_{ij})\right) + \frac{1}{2}\sum_{i\neq j}\varphi_\beta(r_{ij}) \tag{8}$$

In this equation, β_ρ is the factor due to the atomic charge density, and β_φ is the factor due to the presence of particles in the simulation box. Also, F_α is a constant coefficient between 0 and 1. The basis for calculating the thermal conductivity in the following simulations is calculating the flowing heat flux in the atomic samples, estimated using the Green-Kubo method. In Green- Kubo technique, an internalization happens in terms of the selected curve using this formulation [18]:

$$\begin{aligned} J &= \frac{1}{V}\left[\sum_i e_i v_i - \sum_i S_i v_i\right] = \frac{1}{V}\left[\sum_i e_i v_i + \sum_{i<j}(f_{ij}.v_j)x_{ij}\right] \\ &= \frac{1}{V}\left[\sum_i e_i v_i + \frac{1}{2}\sum_{i<j}(f_{ij}.(v_i+v_j))x_{ij}\right] \end{aligned} \tag{9}$$

In Eq. (10), j and i show two fractions at both ends of the bond, S_i is the system entropy, e_i the energy, the force exerted on i and j particles, and V is the total sample volume. The following equation estimates the quantity of thermal conductivity of the simulation box:

$$k = \frac{V}{k_B T^2}\int_0^\infty \langle J_x(0)J_x(t)\rangle dt = \frac{V}{3k_B T^2}\int_0^\infty \langle J(0).J(t)\rangle dt \tag{10}$$

In the above relation, k_B is the Boltzmann constant, V is the occupied volume by the particles in the simulation, $J_x(0)$ is the flowing heat flux in the initial step of the simulation, and $J_x(t)$ is the flowing heat flux at any point in time. In this study, canonical (NVT) and grand canonical (NPT) ensembles are used. Thermostats are used to keep the temperature in a certain range. This procedure controls the flow of thermal energy into or out of the simulated atomic structure [24–26]. In our research, the Nose-Hoover thermostat is used. By applying the Nose-Hoover formulation and considering the motion equations of the Verlet-algorithm, the equations are as follows [25]:

$$r_i(t+dt) = r_i(t) + v_i(t)dt + \frac{1}{2}dt^2\left[\frac{F_i(t)}{m_i} - \xi(t)v_i(t)\right] \tag{11}$$

$$v_i\left(t+\frac{dt}{2}\right) = v_i(t) + \frac{dt}{2}\left[\frac{F_i(t)}{m_i} - \xi(t)v_i(t)\right] \tag{12}$$

$$\xi\left(t+\frac{dt}{2}\right) = \xi(t) + \frac{dt}{2Q}\left[\sum_i^N m_i v_i^2(t) - gk_BT\right] \tag{13}$$

$$\xi(t+dt) = \xi\left(t+\frac{dt}{2}\right) + \frac{dt}{2Q}\left[\sum_i^N m_i v_i^2\left(t+\frac{dt}{2}\right) - gk_BT\right] \tag{14}$$

3. Results and discussion

3.1. Stability of atomic structures

In the first part of this study, physical quantities such as kinetic energy and potential energy of atomic structures in 10 ns are investigated to investigate the equilibrium in the simulated structures. As the time steps in the simulation box increase, the amplitude of kinetic energy oscillation in the simulated samples decreases. As a result, the kinetic energy tends to a constant value. From a quantitative point of view, as shown in Fig. 2, the kinetic energy of the simulated atomic samples tends to 77.02 eV after 10 ns, and as more time steps go by, the numerical value does not change much. The potential energy of simulated atomic structures is one of the most important physical quantities in molecular dynamics simulations. From a computational point of view, this quantity corresponds to the distance between atoms (how atomic structures are arranged) and the used potential in them. According to Fig. 3, the numerical value of this quantity converges to −6769.58 eV, which is visible after 10 ns. Therefore, it can be said that the numerical value of this quantity does not change as more time passes in the simulated atomic samples. From a physical point of view, this convergence in the calculated energy in this part originates from the proper position of atomic structures and the force between atoms that arises from the choice of force field and indicates the equilibrium in atomic structures [18].

After examining the stability of the simulated structures, the combustion process in the structures is investigated. The combustion process will be visible in the atomic sample by applying heat flux (1 Wm^{-2}) to the simulated atomic samples. More precisely, by applying heat flux to the simulated atomic samples, the atomic mobility in these samples increases. With increasing atomic mobility in the simulated samples, mobility and, consequently, the atomic distance increase. With increasing atomic distance, the amount of kinetic energy in the samples increases, and finally, the amount of potential in these structures changes to a positive numerical value. This increasing trend in the amount of potential energy and kinetic energy causes the total energy in atomic structures to increase, corresponding to an increase in temperature, resulting in phase change and combustion in the atomic sample.

3.2. Investigation of thermal behavior of simulated atomic structures

Despite the increase in mobility in atomic samples by applying heat flux, the amount of aluminum nanoparticles was selected so that the aggregating process is not visible in atomic samples. It was found that nanoparticles are very important in determining the

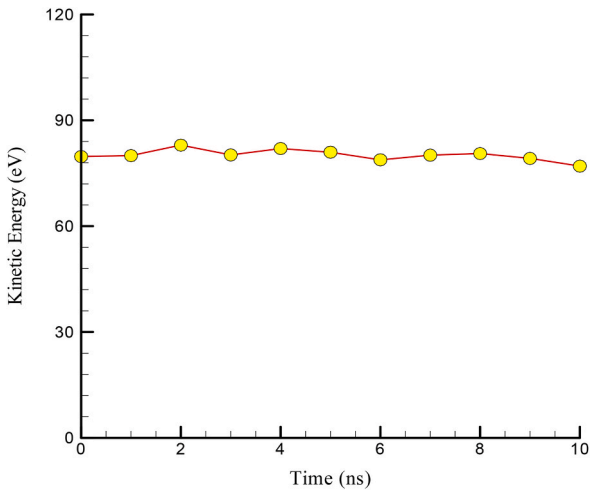

Fig. 2. Change in kinetic energy of the simulated sample.

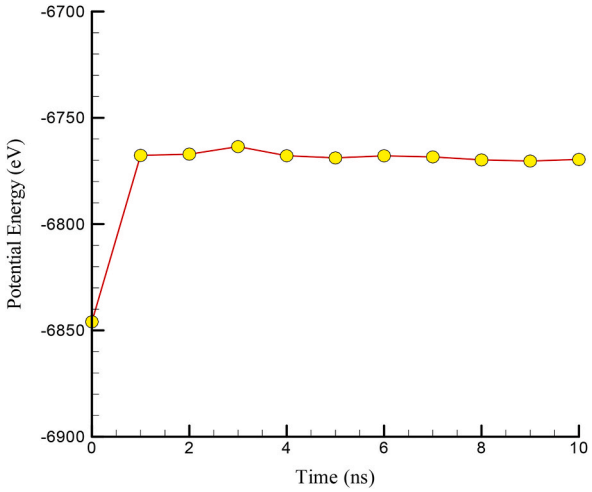

Fig. 3. Change in potential energy of the simulated sample.

properties of systems and structures [27–31]. As a result, the physical behavior of atomic samples is not disturbed. Fig. 4 shows a close-up view of aluminum nanoparticles so that the aggregating process can be seen if present. It should be noted that these images are defined as the output of LAMMPS software after 10 ns (after the application of external heat flux).

After showing how the atomic substitution in the study sample is done, this process is studied numerically. For this purpose, the temperature profile in the simulated samples is checked. Therefore, the thermal properties of simulated nanochannel-fluid/nanofluid systems are investigated by identifying the temperature behavior of the simulated items. In this section, the temperature profiles of the atoms present in the simulated fluid nanofluid are plotted according to the number of bins within the nanochannel in Fig. 5. According to this figure, the temperature behavior of the fluid simulated in this study is similar to their velocity. The temperature profile of the fluid particles in the center of the atomic channel has its highest numerical value. As it approaches the walls of this channel, the numerical value of this quantity decreases.

3.3. Investigation of the effect of temperature on the combustion of atomic structures

As the temperature rises in the simulated atomic samples, the atomic oscillations in the structures increase; with increasing these fluctuations, heat transfer in the samples increases. As a result, the combustion phenomenon in these structures is observed with more intensity. From a computational point of view, with increasing temperature, the number of kinetic energy increases. Finally, this process leads to an increase in potential energy and total energy in the simulated samples. With the increase of expressed energies in atomic structures, the amount of released heat in the simulation box increases. Finally, with increasing temperature to 350 K, the amount of heat flux in atomic samples reaches 12.89 Wm^{-2} (Fig. 6). With the occurrence of the process and so in the atomic samples, the combustion time in the structures also changes and reaches a numerical value of 6.29 ns per initial temperature of 400 K (Fig. 7). An accurate numerical report of heat flux and phase change duration (combustion) in atomic samples with different initial temperature values is presented in Table 1.

Other studies on the heat flux of nanofluids containing aluminum (water/Alumina) show that the heat flux of the nanofluids increases with increasing initial temperature [32,33]. They showed that in the temperature range of 280–350 K, the heat flux changed between 1000 and 1500 Wm^{-2}.

3.4. Investigation of the effect of initial pressure on the combustion of atomic structures

Compared to the initial temperature, pressure has the opposite effect on the combustion process of atomic structures. From the atomic point of view, with increasing pressure in atomic samples, atomic oscillations decrease. As a result, atomic movement and, consequently, atomic mobility in atomic structures decreases. This reduction limits the displacement in the atomic samples, and as a result, changes in potential energy and kinetic energy in these structures are not significant. According to the above explanations, it is expected that with increasing pressure in atomic samples, the amount of generated and transferred heat flux in atomic samples decreases, and as a result, the combustion process is observed in less time. From a numerical point of view and according to the diagram in Fig. 8, the amount of heat flux in the oxygen/aluminum sample increases to a numerical value of 1288 Wm^{-2} (increasing the pressure to a numerical value of 6 bar). On the other hand, according to Fig. 9 and Table 2, the required time for the combustion process in the simulation box decreases to 6.59 ns.

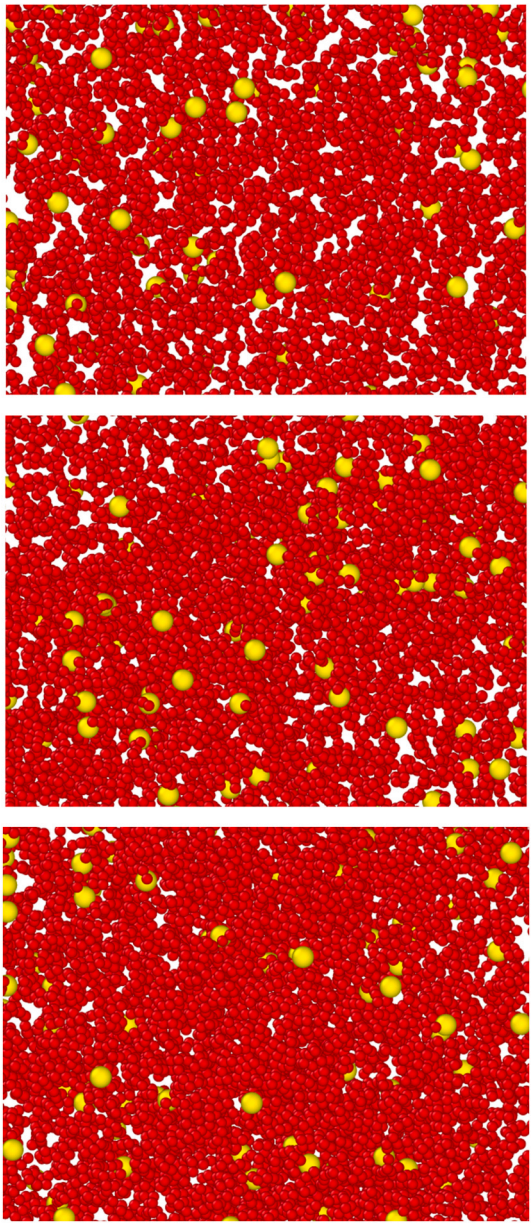

Fig. 4. Close-up of atomic placement in simulated samples to identify aggregations in aluminum nanoparticles.

3.5. Investigation of the effect of external heat flux on the combustion of atomic structures

Increasing the external heat flux in the simulated nanofluid particles inside the copper atomic channel increases the flowing flux in the sample. As the expressed heat flux within the atomic channel increases, the amount of mobility and kinetic energy in the samples increases. As a result, more heat flows into the structures (Fig. 10). This increase reduces the combustion time in atomic samples. According to the reported results in Fig. 11 and Table 3, the combustion time in the simulated samples is reduced to a numerical value of 5.31 ns from a numerical point of view. The results of this part of the research can be used in practical applications. By adding external heat flux, atomic evolution in atomic samples can be intensified. As a result, increasing energy and combustion can be observed in a shorter period, which increases the operational efficiency of the applied samples.

4. Conclusion

This study investigated the thermal behavior and combustion process in a simulated atomic sample with LAMMPS software, including copper channel and oxygen/aluminum nanofluid. In this research, we investigated the effect of temperature, initial pressure,

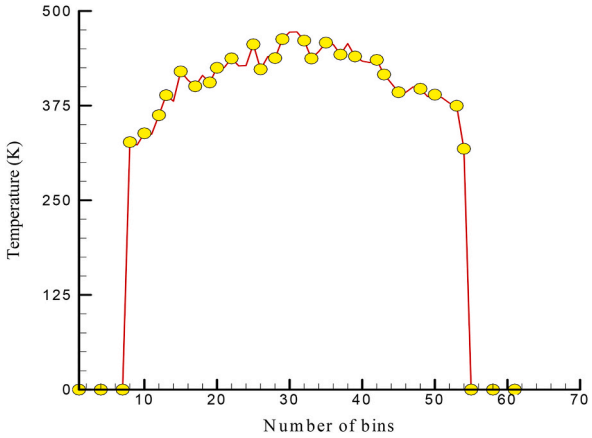

Fig. 5. Temperature profiles within the copper channel.

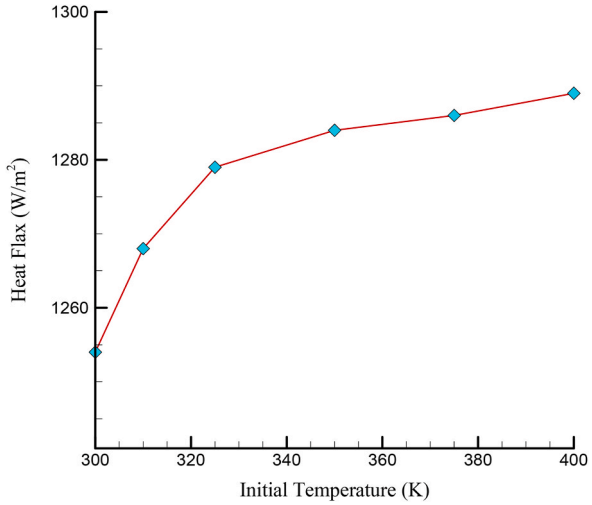

Fig. 6. Heat flux changes in simulated atomic samples versus the initial temperature of atomic structures.

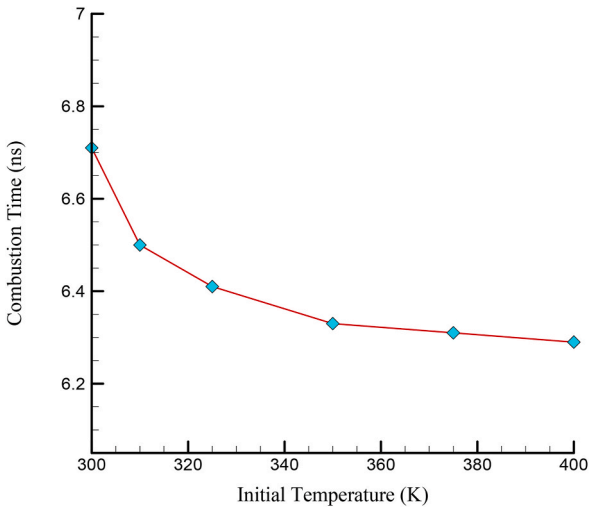

Fig. 7. Combustion time changes in simulated atomic samples versus the initial temperature of atomic structures.

Table 1
Changes related to heat flux and phase change duration in simulated atomic samples according to the initial temperature of atomic structures.

Initial Temperature of Atomic Structures (K)	Heat Flux (Wm^{-2})	Combustion Time (ns)
300	1254	6.71
310	1268	6.50
325	1279	6.41
350	1284	6.33
375	1286	6.31
400	1289	6.29

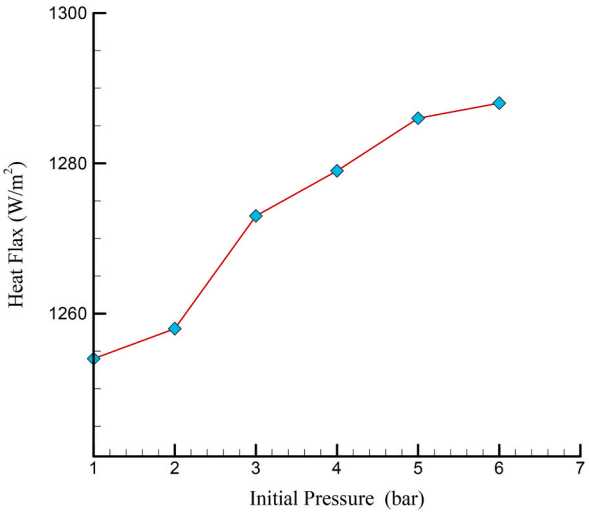

Fig. 8. Heat flux changes in simulated atomic samples in terms of the initial pressure of atomic structures.

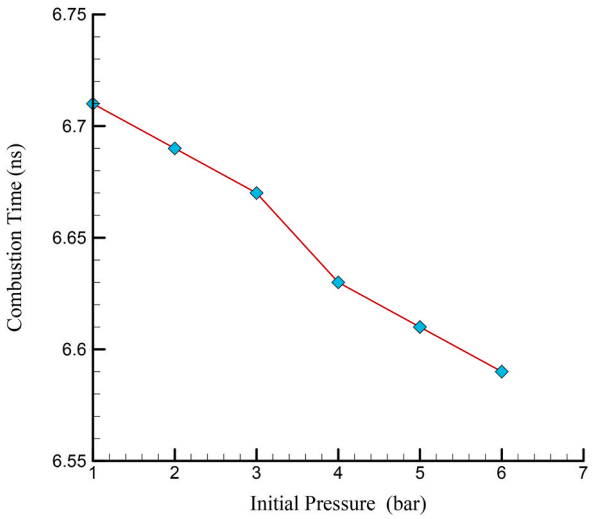

Fig. 9. Combustion time changes in simulated atomic samples in terms of the initial pressure of atomic structures.

and external heat flux on the combustion of atomic structures. In summary, the following results were obtained from this study:

- By examining the physical equilibrium in atomic samples, the amount of kinetic energy in atomic samples was balanced at 77.02 eV. The amount of potential energy in atomic samples was balanced at −6769.58 eV.
- As the initial temperature rises to 350 K, the flux in the atomic sample and the combustion time converged to 1289 Wm^{-2} and 6.29 ns.

Table 2
Changes related to heat flux and phase change duration in simulated atomic samples versus initial pressure of atomic structures.

Initial Pressure of Atomic Structures (bar)	Heat Flux (Wm^{-2})	Combustion Time (ns)
1	1254	6.71
2	1258	6.69
3	1273	6.67
4	1279	6.63
5	1286	6.61
6	1288	6.59

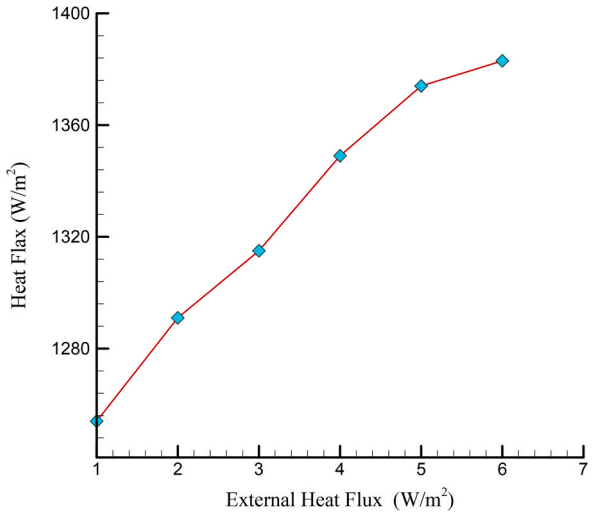

Fig. 10. Heat flux changes in simulated atomic samples in terms of external heat flux.

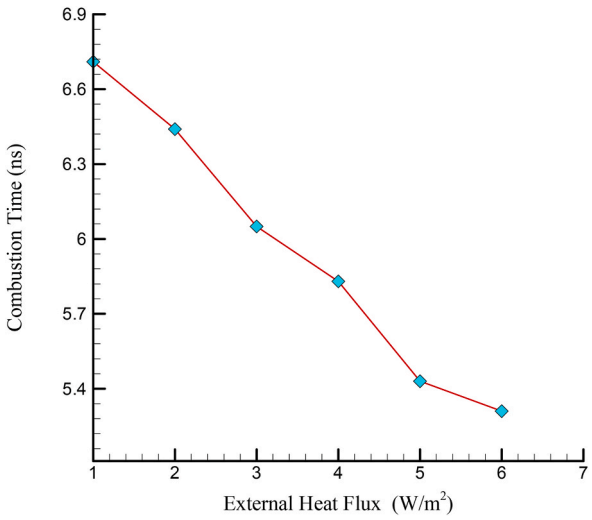

Fig. 11. Combustion time changes in simulated atomic samples in terms of external heat flux.

- By increasing the initial pressure to 5 bar, the flowing flux in the atomic sample and the combustion time converged to 1288 Wm^{-2} and 6.59 ns.
- The flowing flux in the atomic sample and the combustion time converged to 1383 Wm^{-2} and 5. 31 ns with increasing external heat flux.

Table 3
Changes related to heat flux and phase change duration in simulated atomic samples in different external heat fluxes.

External Heat Flux (Wm^{-2})	Flowed Heat Flux (Wm^{-2})	Combustion time (ns)
1	1254	6.71
2	1291	6.44
3	1315	6.05
4	1346	5.83
5	1374	5.43
6	1383	5.31

CRediT authorship contribution statement

Heng Chen: Methodology, Software, Validation, Writing – review & editing, Investigation. **Dmitry Bokov:** Methodology, Software, Validation, Writing – review & editing, Investigation. **Supat Chupradit:** Methodology, Software, Validation, Writing – review & editing, Investigation. **Maboud Hekmatifar:** Methodology, Software, Validation, Investigation. **Mustafa Z. Mahmoud:** Methodology, Software, Validation, Writing – review & editing, Investigation. **Roozbeh Sabetvand:** Methodology, Software, Validation, Writing – original draft, Investigation. **Jinying Duan:** Methodology, Software, Validation, Writing – review & editing, Investigation. **Davood Toghraie:** Methodology, Software, Validation, Writing – original draft, Investigation.

Declaration of competing interest

The authors declare that they have no known competing financial interests or personal relationships that could have appeared to influence the work reported in this paper.

References

[1] D. Toghraie, A.R. Azimian, Molecular dynamics simulation of liquid–vapor phase equilibrium by using the modified Lennard-Jones potential function, Heat Mass Tran. 46 (3) (2010) 287–294.
[2] M. Jourabian, A.A.R. Darzi, D. Toghraie, O.A. Akbari, Melting process in porous media around two hot cylinders: Numerical study using the lattice Boltzmann method, Physica A 509 (2018) 316–335.
[3] S. Oveissi, S.A. Eftekhari, D. Toghraie, Longitudinal vibration and instabilities of carbon nanotubes conveying fluid considering size effects of nanoflow and nanostructure, Physica E 83 (2016) 164–173.
[4] B. Ruhani, D. Toghraie, M. Hekmatifar, M. Hadian, Statistical investigation for developing a new model for rheological behavior of ZnO–Ag (50%–50%)/Water hybrid Newtonian nanofluid using experimental data, Physica A 525 (2019) 741–751.
[5] Y. Zhu, X. Zheng, Y. Lu, X. Yang, A. Kheradmand, Y. Jiang, Efficient upconverting carbon nitride nanotubes for near-infrared-driven photocatalytic hydrogen production, Nanoscale 11 (2019) 20274.
[6] I. Glassman, R.A. Yetter, N.G. Glumac, Combustion, Academic press, 2014.
[7] R.W. Schefer, D. Wicksall, A. Agrawal, Combustion of hydrogen-enriched methane in a lean premixed swirl-stabilized burner, Proc. Combust. Inst. 29 (1) (2002) 843–851.
[8] H. Jung, D.B. Kittelson, M.R. Zachariah, The influence of a cerium additive on ultrafine diesel particle emissions and kinetics of oxidation, Combust. Flame 142 (3) (2005) 276–288.
[9] Q. Kong, H. Zhang, L. Zheng, D.Y. Wang, J. Zhang, Effect on thermal and combustion behaviors of montmorillonite intercalation nickel compounds in polypropylene/IFR system, Polym. Adv. Technol. 28 (8) (2017) 965–970.
[10] C. Allen, G. Mittal, C.-J. Sung, E. Toulson, T. Lee, An aerosol rapid compression machine for studying energetic-nanoparticle-enhanced combustion of liquid fuels, Proc. Combust. Inst. 33 (2) (2011) 3367–3374.
[11] J. Sun, R. Dobashi, T. Hirano, Structure of flames propagating through aluminum particles cloud and combustion process of particles, J. Loss Prev. Process. Ind. 19 (6) (2006) 769–773.
[12] H. Tyagi, P.E. Phelan, R. Prasher, R. Peck, T. Lee, J.R. Pacheco, P. Arentzen, Increased hot-plate ignition probability for nanoparticle-laden diesel fuel, Nano Lett. 8 (5) (2008) 1410–1416.
[13] S. Hong, A.C. van Duin, Molecular dynamics simulations of the oxidation of aluminum nanoparticles using the ReaxFF reactive force field, J. Phys. Chem. C 119 (31) (2015) 17876–17886.
[14] G. Li, L. Niu, W. Hao, Y. Liu, C. Zhang, Atomistic insight into the microexplosion-accelerated oxidation process of molten aluminum nanoparticles, Combust. Flame 214 (2020) 238–250.
[15] V. Baijot, D.-R. Mehdi, C. Rossi, A. Esteve, A multi-phase micro-kinetic model for simulating aluminum based thermite reactions, Combust. Flame 180 (2017) 10–19.
[16] M. Bidabadi, M.V. Bozorg, V. Bordbar, A three-dimensional simulation of discrete combustion of randomly dispersed micron-aluminum particle dust cloud and applying genetic algorithm to obtain the flame front, Energy 140 (2017) 804–817.
[17] M. Amini, A.S.A. Ramazani, S.A. Haddadi, A. Kheradmand, Mechanical, rheological and oxygen barrier properties of ethylene vinyl acetate/diamond nanocomposites for packaging applications, Diam. Relat. Mater. 99 (2019) 107523.
[18] D.C. Rapaport, The Art of Molecular Dynamics Simulation, Cambridge university press, 2004.
[19] L. Verlet, "Computer" experiments" on classical fluids. I. Thermodynamical properties of Lennard-Jones molecules, Phys. Rev. 159 (1) (1967) 98.
[20] D.W. Brenner, The art and science of an analytic potential, Phys. Status Solidi 217 (1) (2000) 23–40.
[21] J.E. Lennard-Jones, Cohesion, Proc. Phys. Soc. 43 (5) (1931) 461, 1926-1948.
[22] S.L. Mayo, B.D. Olafson, W.A. Goddard, DREIDING: a generic force field for molecular simulations, J. Phys. Chem. 94 (26) (1990) 8897–8909.
[23] D. Halliday, R. Resnick, J. Walker, Fundamentals of Physics, John Wiley & Sons, 2013.
[24] H.J. Berendsen, D. van der Spoel, R. van Drunen, GROMACS: a message-passing parallel molecular dynamics implementation, Comput. Phys. Commun. 91 (1–3) (1995) 43–56.
[25] S. Nosé, A unified formulation of the constant temperature molecular dynamics methods, J. Chem. Phys. 81 (1) (1984) 511–519.
[26] A. Kheradmand, A. Wainwright, L. Wang, Y. Jiang, Anchoring iron oxides on carbon nitride nanotubes for improved photocatalytic hydrogen production, Energy Fuels 35 (2021) 868.

[27] Al-Shawi Sarmad Ghazi, et al., Synthesis of NiO nanoparticles and sulfur, and nitrogen co doped-graphene quantum Dots/NiO nanocomposites for antibacterial application, J. Nanostruct. 11 (1) (2021) 181–188.
[28] A. Emrani, A. Davoodnia, N. Tavakoli-Hoseini, Alumina supported ammonium dihydrogenphosphate (NH 4 H 2 PO 4/Al 2 O 3): Preparation, characterization and its application as catalyst in the synthesis of 1, 2, 4, 5-tetrasubstituted imidazoles, Bull. Korean. Chem. Soc. 32 (7) (2011) 2385–2390.
[29] N. Ngafwan, et al., Study on novel fluorescent carbon nanomaterials in food analysis, Food Sci. Technol. (2021), https://doi.org/10.1590/fst.37821.
[30] T. Tjahjono, M. Elveny, S. Chupradit, D. Bokov, H. Hoi, M. Pandey, Role of cryogenic cycling rejuvenation on flow behavior of ZrCuAlNiAg metallic glass at relaxation temperature, Trans. Indian Inst. Met. (2021) 1–7.
[31] S. Pathirana, D. Asirvatham, M.G.M. Johar, An agent based approach for electroencephalographic data classification, in: In 2018 13th International Conference on Computer Science & Education (ICCSE), 2018, pp. 248–252.
[32] J. Ham, H. Kim, Y. Shin, H. Cho, Experimental investigation of pool boiling characteristics in Al_2O_3 nanofluid according to surface roughness and concentration, Int. J. Therm. Sci. 114 (2017) 86–97.
[33] Z. Shahmoradi, N. Etesami, M.N. Esfahany, Pool boiling characteristics of nanofluid on flat plate based on heater surface analysis, Int. Commun. Heat Mass Tran. 47 (2013) 113–120.